Glyphosate-Based Herbicides Produce Teratogenic Effects on Vertebrates by Impairing Retinoic Acid Signaling

Alejandra Paganelli, Victoria Gnazzo, Helena Acosta, Silvia L. López, and
Andrés E. Carrasco*

*Laboratorio de Embriología Molecular, CONICET-UBA, Facultad de Medicina, Universidad de Buenos Aires,
Paraguay 2155, 3° piso (1121), Ciudad Autónoma de Buenos Aires, Argentina*

The broad spectrum herbicide glyphosate is widely used in agriculture worldwide. There has been ongoing controversy regarding the possible adverse effects of glyphosate on the environment and on human health. Reports of neural defects and craniofacial malformations from regions where glyphosate-based herbicides (GBH) are used led us to undertake an embryological approach to explore the effects of low doses of glyphosate in development. *Xenopus laevis* embryos were incubated with 1/5000 dilutions of a commercial GBH. The treated embryos were highly abnormal with marked alterations in cephalic and neural crest development and shortening of the anterior−posterior (A-P) axis. Alterations on neural crest markers were later correlated with deformities in the cranial cartilages at tadpole stages. Embryos injected with pure glyphosate showed very similar phenotypes. Moreover, GBH produced similar effects in chicken embryos, showing a gradual loss of rhombomere domains, reduction of the optic vesicles, and microcephaly. This suggests that glyphosate itself was responsible for the phenotypes observed, rather than a surfactant or other component of the commercial formulation. A reporter gene assay revealed that GBH treatment increased endogenous retinoic acid (RA) activity in *Xenopus* embryos and cotreatment with a RA antagonist rescued the teratogenic effects of the GBH. Therefore, we conclude that the phenotypes produced by GBH are mainly a consequence of the increase of endogenous retinoid activity. This is consistent with the decrease of Sonic hedgehog (Shh) signaling from the embryonic dorsal midline, with the inhibition of *otx2* expression and with the disruption of cephalic neural crest development. The direct effect of glyphosate on early mechanisms of morphogenesis in vertebrate embryos opens concerns about the clinical findings from human offspring in populations exposed to GBH in agricultural fields.

Introduction

The broad-spectrum glyphosate based herbicides (GBHs) are widely used in agricultural practice, particularly in association with genetically modified organisms (GMO) engineered to be glyphosate resistant such as soy crops. Considering the wide use of GBH/GMO agriculture, studies of the possible impacts of GBH on environmental and human health are timely and important. Given the intensive use of this technological package in South America, studies of the possible impacts on environment and human health are absolutely necessary, together with adequate epidemiological studies. The need for information about the developmental impact of GBH is reinforced by a variety of adverse health effects on people living in areas where GBH is extensively used, particularly since there is a paucity of data regarding chronic exposure to sublethal doses during embryonic development.

It is important to note that the bulk of the data provided during the evaluation stages of GBH/GMO safety were provided by the industry. Given the recent history of the endocrine disruptor field with low dose effects observed in numerous academic laboratories but not in industry-funded studies (*1, 2*), it is clear that a reasonable corpus of independent studies is necessary to fully evaluate the effects of agrochemicals on human health. This is particularly important when significant economic interests are concerned.

There is growing evidence raising concerns about the effects of GBH on people living in areas where herbicides are intensively used. Women exposed during pregnancy to herbicides delivered offspring with congenital malformations, including microcephaly, anencephaly, and cranial malformations (*3*).

Relevant contributions to the subject were made by Seralini's group, among others (*4*). They showed that a GBH acts as an endocrine disruptor in cultures of JEG3 placental cells, decreasing the mRNA levels of the enzyme CYP19 (an essential component of cytochrome p450 aromatase) and inhibiting its activity. CYP19 is responsible for the irreversible conversion of androgens into estrogens. The GBH Roundup is able to disrupt aromatase activity. Importantly, the active principle glyphosate interacts with the active site of the purified enzyme and its effects in cell cultures, and microsomes are facilitated by other components in the Roundup formulation that presumably increase the bioavailability of glyphosate (*4*). Glyphosate penetration through the cell membrane and subsequent intracellular action is greatly facilitated by adjuvants such as surfactants (*5, 6*).

In addition, both glyphosate and the commercial herbicide severely affect embryonic and placental cells, producing mitochondrial damage, necrosis, and programmed cell death by the activation of caspases 3/7 in cell culture within 24 h with doses far below those used in agriculture. Other effects observed include cytotoxicity and genotoxicity, endocrine disruption of the androgen and estrogen receptors, and DNA damage in cell lines (*7, 8*).

* Corresponding author. Phone: +5411 5950 9500 ext. 2216. Fax: +5411 5950 9626. E-mail: acarrasco@fmed.uba.ar.

More recently, rats fed with a glyphosate-resistant genetically modified corn showed functional alterations in two detoxificant organs: kidney and liver, and the heart and the hematopoietic system (*9*).

Another line of evidence supporting adverse effects of glyphosate was provided by Bellé's group. They suggested that glyphosate and its principal metabolite, AMPA, alter cell cycle checkpoints by interfering with the physiological DNA repair machinery. Several GBHs were assayed, and they induced cell-cycle dysfunction from the first cell division in sea urchin embryos (*10, 11*). The threshold concentration for this effect is 500- to 4000-fold lower than that sprayed on crops in the field. Eight millimolar glyphosate induces a delay in the kinetics of the first cell cleavage of sea urchins, altering the entry into S-phase by interfering with the activation of the CDK1/cyclin B complex (*6, 12*). This failure of cell-cycle checkpoints is known to lead to genomic instability and the possible development of cancer. In agreement with these findings, genotoxicity studies of glyphosate or its metabolites suggest that the irreversible damage in the DNA may increase the risk of carcinogenesis (*13, 14*).

Aside from the previously reported teratogenic effects of glyphosate-based formulations on cephalic structures in amphibians (*15*), there is almost no information available about the molecular mechanisms associated with GBH or glyphosate teratogenesis. Reports of neural defects and craniofacial malformations from regions where GBHs are used heavily led us to an embryological approach to explore the effects of low doses of glyphosate in *Xenopus* and chicken embryogenesis.

We show here that sublethal doses are sufficient to induce reproducible malformations in *Xenopus* and chicken embryos treated with a 1/5000 dilution of a GBH formulation (equivalent to 430 μM of glyphosate) or in frog embryos injected with glyphosate alone (between 8 and 12 μM per injected cell). GBH treated or glyphosate injected frog embryos showed very similar phenotypes, including shortening of the trunk, cephalic reduction, microphthalmy, cyclopia, reduction of the neural crest territory at neurula stages, and craniofacial malformations at tadpole stages. These defects suggested a link with the retinoic acid (RA) signaling pathway. Reporter gene assays using a RA-dependent reporter revealed that GBH treatment increases endogenous RA activity. Strikingly, we demonstrate that Ro 41-5253 (Ro), an antagonist of RA (*16, 17*), rescues the phenotype produced by GBH. We propose that at least some of the teratogenic effects of GBH are mediated by increased endogenous RA activity in the embryos. This is consistent with the very well-known syndrome produced by an excess of RA, as described by the epidemiological study of Lammer et al. in humans (*18*) and in vertebrate embryos (*19–25*).

Experimental Procedures

Embryo Culture and Treatments. *Xenopus laevis* embryos were obtained by in vitro fertilization, incubated in $0.1\times$ modified Barth's saline (MBS) (*26*) and staged according to Nieuwkoop and Faber (*27*). The GBH used was Roundup Classic (Monsanto), containing 48% w/v of a glyphosate salt. Treatments were performed from the 2-cell stage with GBH dilutions of 1/3000, 1/4000, and 1/5000 prepared in $0.1\times$ MBS. For rescue experiments, 0.5 or 1 μM Ro-415253 was added at stage 9. Cyclopamine (Sigma C4116) was used at 100 μM concentration in $0.1\times$ MBS and was applied from the 2-cell stage until fixation. Embryos were fixed in MEMFA (*28*) when sibling controls reached the desired stage.

***Xenopus* Embryo Injections, Whole Mount in Situ Hybridization and Cartilage Staining.** Embryos were injected with 360 or 500 pg of glyphosate (*N*-(phosphonomethyl) glycine (Sigma

337757) per cell into one or both cells at the 2-cell stage. Glyphosate was coinjected with 10 ng of Dextran Oregon Green (DOG, Molecular Probes) to identify the injected side as previously described (*29*). Embryos were cultured in $0.1\times$ MBS and fixed in MEMFA when sibling controls reached the desired stage. Whole-mount in situ hybridization (WMISH) with digoxigenin-labeled antisense RNA probes was performed as previously described (*30*) except that the proteinase K step was omitted. For cartilage visualization, embryos were fixed in MEMFA at stages 45–47, washed with PBS, and stained overnight in 0.04% Alcian blue, 20% acetic acid, and 80% ethanol. After extensive washing with ethanol and bleaching with 2% KOH, embryos were washed with 20% glycerol and 2% KOH, and dehydrated through a glycerol/2% KOH series until 80% glycerol was reached.

Detection of RA Activity. Embryos were injected into one cell at the 2-cell stage with 320 pg of the plasmid RAREhplacZ (RAREZ) (*31, 32*) and placed immediately in 1/3000, 1/4000, and 1/5000 GBH dilutions. Basal luminiscence was detected in uninjected and untreated embryos. The endogenous RA activity was measured in embryos injected with RAREZ and left untreated. As positive controls, embryos were injected with the RAREZ plasmid and incubated at late blastula stage with 0.5 or 5 μM all-*trans*-retinoic acid (RA, Sigma R2625). For rescue experiments, embryos injected with the reporter plasmid were incubated in a 1/4000 dilution of GBH from the 2-cell stage, and when they reached the blastula stage, 1 μM of Ro 41-5253 was added. Finally, when sibling controls reached the neurula stages (*14, 15*), all embryos were processed for chemiluminiscent quantitation of the reporter activity by using the β-gal reporter gene assay (Roche). Protein extracts and enzymatic reactions were performed as previously reported (*33*). Luminiscence was measured on duplicate samples in FlexStation 3 equipment (Molecular Devices), and values were normalized by protein content (*32*). A two-tailed *t* test was employed to analyze the significance in the difference of the means. The experiment was repeated three times.

Treatments of Chicken Embryos. After opening a small window in the shell, fertilized chicken eggs (White Leghorn strain) were injected above the air chamber in the inner membrane with 20 μL of 1/3500 or 1/4500 dilutions of GBH. Control embryos were injected only with 20 μL of H_2O. After injection, the window was sealed with transparent adhesive tape, and eggs were placed with their blunt end up at room temperature for 30 min. Then, eggs were incubated in darkness at 38 °C in a humidified incubator (56–58% humidity) and rotated at regular intervals. After appropriate incubation times, embryos were isolated and staged according to Hamburger and Hamilton (*34*).

Whole-Mount Inmunofluorescence and WMISH of Chicken Embryos. Embryos were fixed 2–4 h in freshly prepared 4% paraformaldehyde, rinsed, and processed for analysis. For immunofluorescence, embryos were blocked overnight at 4 °C in blocking solution (5% normal goat serum, 0.3% Triton X-100, 0.01% NaN3, and Tris buffer saline (TBS) at pH 7.4). Then, they were incubated with a 1/50 dilution of a mouse anti-Pax6 monoclonal primary antibody (Developmental Hybridoma Bank) in TBS at pH 7.4 and 0.3% Triton X-100 for 48 h at 4 °C. Embryos were washed three times with TBS and incubated at 4 °C with the secondary antibody (1/1000 fluorescein-conjugated (FITC) antimouse IgG, Jackson ImmunoResearch) in TBS at pH 7.4, 0.3% Triton X-100, and 3% normal goat serum for at least 12 h. Finally, embryos were washed with TBS, placed in a glass culture dish with 80% v/v of glycerol in water, and photographed. WMISH was performed as described for *Xenopus* embryos, using a *c-shh* probe.

Results

GBH and Glyphosate Alter Neural Crest Markers, Rhombomeric Patterning, and Primary Neuron Differentiation. In order to examine whether GBH treatment can affect neural crest development, rhombomeric patterning, and neuronal differentiation, 2-cell stage *Xenopus laevis* embryos were
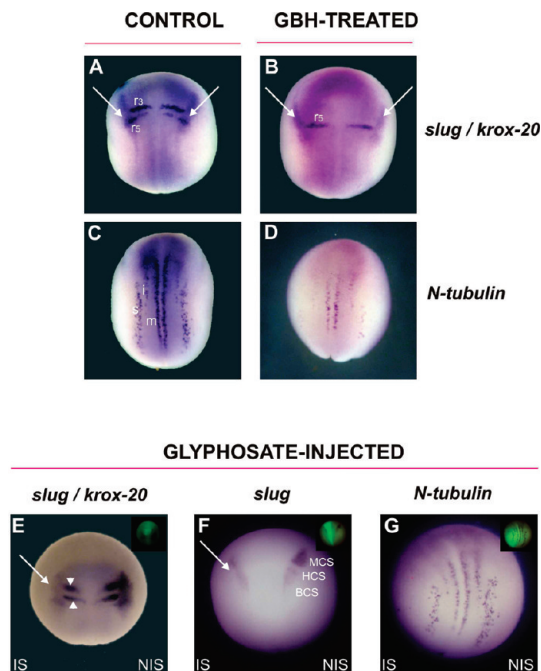
CONTROL **GBH-TREATED**

GLYPHOSATE-INJECTED

slug / krox-20 *slug* *N-tubulin*

Figure 1. GBH and glyphosate disturb neural crest formation, rhombomeric patterning and primary neuron differentiation. (A–G) Embryos were analyzed at neurula stage by WMISH with different markers. All are dorsal views (anterior is up). (A,C) Control embryos. (B,D) Embryos treated with 1/5000 dilution of GBH. (B) Impairment of neural crest formation as revealed by the specific marker *slug* (arrows). Notice the down-regulation of the *krox-20* domain in the r3 rhombomere. *Slug* and *krox-20* were down-regulated in 87% of treated embryos ($n = 30$). (D) Suppression of primary neuron formation as seen with the differentiation marker *N-tubulin*. The number of primary neurons was decreased in 83% of treated embryos ($n = 30$). (E–G) Embryos unilaterally injected with 500 pg of glyphosate per cell plus DOG as the tracer. The injected side is demarcated by the green fluorescence in the insets and is oriented to the left. IS, injected side. NIS, noninjected side. (E,F) Abolishment of *slug* expression in the cranial neural crest domains (arrow; 77%, $n = 31$) and diminution of *krox-20* expression in r3 and r5 (arrowheads; 71%, $n = 21$) on the IS. (G) Reduction of *N-tubulin* expression on the IS (81%, $n = 16$). r3, is the third rhombomere; r5, fifth rhombomere. m, i, and s, are primary motor neurons, interneurons, and sensory neurons, respectively. MCS, HCS, and BCS, are mandibular crest segment, hyoid crest segment, and branchial crest segment, respectively.

exposed to GBH, as described in Experimental Procedures, and assayed by whole mount in situ hybridization (WMISH) at the neurula stage (stage 14–15). The neural crest marker *slug* begins its expression early, where neural crest induction takes place. At neurula stage, it is expressed in the neural crest territory (Figure 1A, arrows) (*35*). Treated embryos show an important down-regulation of *slug* in the neural crest territory (Figure 1B, arrows) in comparison with that of sibling controls. To study the effects on hindbrain patterning, we analyzed the expression of *krox-20*. This zinc finger transcription factor is expressed in rhombomeres r3 and r5 (Figure 1A) and has been shown to play an important role in controlling rhombomere identity (*36*). The r3 stripe was lost in GBH-treated embryos (Figure 1B). This resembles the progressive loss from anterior to posterior rhombomeres associated with increasing concentrations of RA treatments in *Xenopus* and mouse embryos (*37, 38*).

Then we investigated primary neurogenesis at the neural plate stage. At this time, *N-tubulin* is normally expressed in differentiated primary neurons organized in three longitudinal domains in the posterior neural plate: medial, intermediate, and lateral, which correspond to motor neurons (m), interneurons (i), and sensory neurons (s), respectively (Figure 1C) (*39*).

Treated embryos showed a down-regulation in the three stripes of primary neurons (Figure 1D).

To corroborate if the effect is specifically due to the active principle of the herbicide and not to adjuvants present in formulations, glyphosate was injected into one cell at the 2-cell stage and *slug*, *krox-20*, and *N-tubulin* were revealed at stages 14–15, as before. These embryos showed an important down-regulation of *slug* (Figure 1E, arrow), resembling the effects of GBH on this marker at this stage of development. Although *Krox-20* did not completely disappear from r3 as in GBH-treated embryos, the expression clearly decreased in this rhombomere as well as in r5, indicating that glyphosate also alters rhombomeric patterning (Figure 1E; arrowheads).

Normally, at stage 18, the neural crest has formed three premigratory blocks from which three different segments segregate: mandibular crest segment, hyoid crest segment, and branchial crest segment (MCS, HCS, and BCS; Figure 1F). The first segment contributes to the Meckel, quadrate, and ethmoid-trabecular cartilages; the hyoid crest segment to the ceratohyal cartilage, and the branchial segment to the cartilages of the gills (*40*). Glyphosate-injected embryos showed that the segregation process clearly affected the injected side (Figure 1F, arrow), suggesting that the derived cartilages may be affected at later stages during development. When hybridized with *N-tubulin*, these embryos showed a decrease in the number of primary neurons in the three stripes corresponding to motor neurons, interneurons, and sensory neurons (Figure 1G, arrows), resembling the effects of GBH treatments, although with milder consequences for this marker.

In conclusion, the effects of GBH-treated and glyphosate-injected embryos represent equivalent phenotypes despite the fact that they are not identical. The adjuvant present in the commercial formulation may explain the differences. Taken together, these results indicate that both GBH and glyphosate impair neuronal differentiation, rhombomeric formation, and the pattern of the neural crest during induction and segregation.

GBH and Glyphosate Produce Head Defects and Impair the Expression of Dorsal Midline and Cephalic Markers. Because craniofacial defects were observed in humans residing in areas chronically exposed to GBH, we decided to explore whether genes involved in head development are altered as a consequence of treatment with GBH or injection of glyphosate. Shh acts as a morphogen controlling multiple developmental processes. During early vertebrate embryogenesis, *shh* expressed in midline structures such as the notochord, prechordal mesoderm, and floor plate controls left–right asymmetry, neuron identity, neural survival, and dorso-ventral patterning of the neural tube (*41, 42*). Moreover, Shh secreted by the prechordal mesoderm is responsible for resolving the brain and the retina field into two separate hemispheres and eyes, preventing cyclopia (*43*).

Shh expression was dramatically reduced in the dorsal midline at neurula stages, especially in the prechordal mesoderm in GBH-treated embryos. The anterior limit of the *shh* expression domain is moved caudally in treated embryos, in relation to the *pax6* domain (compare green arrowheads, Figure 2A–C).

Pax6 is essential for eye formation in a wide range of species. It is expressed in the eye primordia of vertebrates such as the mouse, chicken, *Xenopus*, zebrafish, and humans, as well as in invertebrates such as *Drosophila* (*44–47*). Embryos incubated with GBH showed a distinct down-regulation of the *pax6* territory (compare white arrowheads; Figure 2A–C). Moreover, in treated embryos, the *pax6* domain is not divided in the eye field (light blue arrowheads; Figure 2B,C). These results suggest
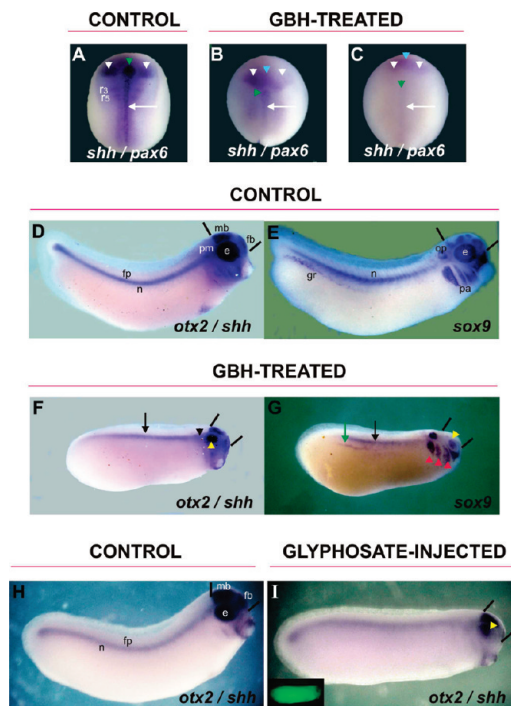
Figure 2. GBH and glyphosate produce A-P truncations and impair the expression of dorsal midline and neural crest markers. (A−I) WMISH analysis at neurula (A−C) and tailbud (D−I) stages. (A) Control embryo hybridized with *shh* (arrow) and *pax6* (white arrowheads). (B−C) Embryos exposed to 1/5000 dilution of GBH. Notice the dramatic reduction of *shh* expression in the embryonic dorsal midline (arrows) and the caudal displacement of the anterior limit (green arrowheads) (85%, $n = 33$). The expression of *pax6* is reduced, and the domain is not properly resolved in the eye field (light blue arrowheads) (85%, $n = 33$). (D,E) Control embryos. (D) Normal expression of *shh* in the notochord (n), floor plate (fp), and prechordal mesoderm (pm) and of *otx2* in the eye (e), forebrain (fb), and midbrain (mb). The space between bars indicates the size of the brain. (E) Normal expression of *sox9* in the pharyngeal arches (pa), otic placode (op), eye (e), genital ridge (gr), and notochord (n). (F,G) 1/5000 GBH-treated embryos. (F) Reduced expression of *shh* and *otx2* (92%, $n = 24$) in dorsal midline cells (*shh*, arrow), prechordal mesoderm (*shh*, black arrowhead), eye (*otx2*, yellow arrowhead), and brain structures (*otx2*, space between bars). (G) Diminution of *sox9* expression in the notochord (black arrow), genital ridge (green arrow), and eyes (yellow arrowhead) (87%, $n = 30$). Notice the delay in the migration of neural crest cells toward the pharyngeal arches (red arrowheads). Treated embryos (F and G) showed microphtalmy, microcephaly (compare the space between bars in D−G), and a shortened A-P axis (89%, $n = 54$). (H,I) Embryos hybridized with *shh* and *otx2*. (H) Control embryo showing the same structures as those in D. (I) Embryo bilaterally injected with 360 pg of glyphosate per cell at the 2-cell stage plus DOG as tracer (green fluorescence in the inset). Similar to that in GBH-treated embryos, *shh* and *otx2* expression was reduced (62%, $n = 16$), and this was accompanied by microcephaly (compare space between bars) and microphtalmy (yellow arrowhead).

that a down-regulation of *shh* expression in the prechordal mesoderm together with a diminution of *pax6* expression may underlie the defects in the resolution of the retina field and the brain hemispheres in embryos treated with GBH.

To test whether these molecular alterations were associated with defects at later stages, we analyzed the expression of *shh/otx2* (Figure 2D,F) and *sox9* (Figure 2E,G) in embryos treated with GBH as before but fixed at tailbud stages. *Otx2* is a homeobox-containing gene expressed in retinal and lens components of the eye and telencephalic, diencephalic, and mesencephalic regions and plays an important role in specifying anterior structures (*48, 49*). Exposed embryos showed a decrease of anterior *shh* expression with concomitant microphtalmy and microcephaly, as revealed by the reduction of the *otx2* domain

(Figure 2, compare the space between bars in the control embryo in D with the treated embryo in F). Also, there is a pronounced shortening of the A-P axis (compare control embryos in Figure 2D,E with treated embryos in F,G). In control embryos, the transcription factor *sox9* is expressed in the cranial neural crest cells as they populate the pharyngeal arches, the otic placode, the developing eye, the genital ridges, and also the notochord (Figure 2E) (*50*). Embryos treated with GBH showed reduced eyes and genital ridges, and developed abnormal pharyngeal arches. The migration of neural crest cells to these structures was delayed, as revealed by a more dorsal position (compare Figure 2G with E).

To analyze the effects of glyphosate alone on dorsal midline development, we performed bilateral injections at the 2-cell stage. Embryos were fixed when sibling controls reached stage 28−30, and the expression of *shh* was analyzed. To better understand cephalic defects, the pattern of *otx2* was also examined. Similar to embryos treated with GBH, we observed reduced prechordal *shh* expression accompanied by strong microcephalic and microphtalmic phenotypes. This is likely due to a decrease of midline-derived signals (Figure 2H,I). Taken together, all of these results indicate that GBH as well as glyphosate alone cause cephalic defects that probably result from a reduction of *shh* and *otx2* expression in anterior structures. The delay in the migration of cranial neural crest cells in the tailbud stage embryos together with the inhibition of *slug* expression at earlier stages led us to next examine whether craniofacial development would be impaired in older embryos.

GBH and Glyphosate Disrupt the Development of the Craniofacial Skeleton. The pattern of neural crest derivatives in the cranial skeleton of the *Xenopus* embryo was previously established (*40*). Briefly, in the first pharyngeal arch, neural crest cells contribute to the upper (quadrate, Qu) and lower (Meckel's, Me) jaws; in the second arch, they contribute to the cerathoyal cartilage (Ce), while in the third and fourth arches, neural crest cells contribute to the anterior and posterior regions of the branchial/gills cartilage (Br), respectively (Figure 3C).

To address if the effects seen at neurula and tailbud stages are correlated with craniofacial malformations, embryos treated with GBH and embryos unilaterally or bilaterally injected with glyphosate at the 2-cell stage were allowed to develop up to stage 47 and processed with Alcian Blue staining for skeletal analysis. The gross morphology of GBH-treated embryos revealed an overall reduction of cranial structures and microphtalmy (compare Figure 3A,C with B,D). All affected embryos displayed a reduction of the quadrate and Meckel's cartilages (asterisks, Figure 3D), while the branchial and cerathoyal cartilages were mildly affected.

Unilateral glyphosate injections resulted in a general decrease of Alcian blue staining and in a reduction of the Meckel's and quadrate cartilages on the injected side (asterisks, Figure 3E,F). In some embryos, the eye practically disappeared from the injected side (arrow, Figure 3H). Moreover, bilaterally injected embryos exhibited cyclopia (Figure 3I, arrow), consistent with the loss of Shh signaling from the prechordal mesoderm observed at earlier stages. Similar results were obtained in frog embryos treated with cyclopamine (Figure 3J), a known inhibitor of the Hedgehog pathway which leads to developmental malformations and holoprosencephaly-like abnormalities, including cyclopia in the most severe cases (*51−53*). Unilateral injections of cyclopamine produced cartilage alterations similar to those obtained with glyphosate injections (not shown).

In summary, our results are compatible with the malformations observed in the offspring of women chronically exposed
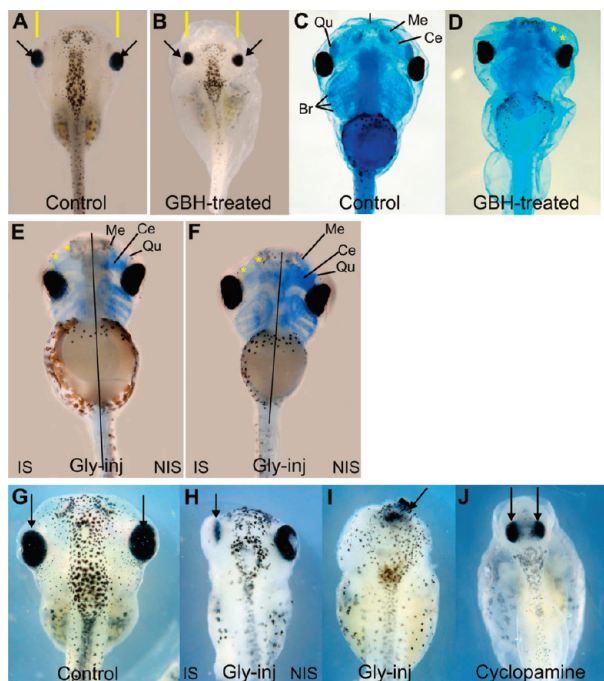
Figure 3. GBH treatment and glyphosate injection result in cephalic malformations and abnormal development of the craniofacial skeleton. (A−D) 1/5000 GBH-treated embryos analyzed at stage 45−47. (A,B) Gross morphology. (A) Control embryo; eyes (arrows); head size (space between yellow bars). (B) Embryo exposed to GBH showing reduced eyes (arrows) and head structures (89%, n = 38) (compare the space between yellow bars in A and B). (C,D) Embryos stained with Alcian blue. (C) Control embryo, showing facial cartilages: Meckel (Me), ceratohyal (Ce), infrarrostral (I), quadrato (Qu), and branchial (Br). (D) Reduction of Me and Qu cartilages (asterisks) in GBH-exposed embryos (77%, n = 39). (E−I) Embryos injected with 360 pg of glyphosate per cell in one or both cells at the 2-cell stage and analyzed at stage 47 by Alcian blue staining (E,F) or gross morphology (H,I), which was compared with that of sibling controls (G). (E,F) Unilaterally injected embryos showing reduced Alcian blue staining and smaller Qu and Me cartilages (asterisks) on the IS (56%, n = 16). (G) Control embryo. Arrows indicate the position of the eyes. (H) Notice the reduction of the eye in the IS (arrow) (54%, n = 13). (I) Bilaterally injected embryo exhibiting cyclopia (arrow) (38%, n = 8). (J) Cyclopamine-treated embryo. Observe the proximity of both eyes (arrows), due to midline defects (compare with the control embryo in G). IS, injected side. NIS, noninjected side. Gly-inj, embryo injected with glyphosate.

to GBH during pregnancy (see Discussion). These malformations suggest the loss of midline signaling, accompanied by defects in neural crest migration (or increased apoptosis) with aberrant development of mandibular and maxillary structures.

Phenotype Induced by GBH Is at Least Mediated by Changes in RA Signaling. It was previously reported that increasing concentrations of RA caused progressive truncation of anterior and posterior structures in *Xenopus laevis* (20, 21). The most severely affected embryos lacked eyes, nasal pits, forebrain, midbrain, and otic vesicles, and displayed truncations of the tail. The phenotypes produced by GBH and glyphosate resemble the teratogenic effects of embryos treated with RA; therefore, we theorized that the RA pathway could be associated with the morphogenetic effects of glyphosate during early embryogenesis.

The RA signal is transduced through nuclear retinoic acid receptors (RARs), which control the expression of target genes involved in vertebrate pattern formation, organogenesis, and tissue homeostasis (54). Ro 41-5253 (Ro) is an antagonist of the RARα receptor, which is expressed during early development in *Xenopus* (16, 17, 55, 56). Ro was previously used as a

tool to block retinoid-mediated signaling, producing a variety of morphological changes in the frog embryo. The most severe phenotypes showed anterior and posterior truncations, a reduction or loss of eyes and otic vesicles, and a general disorganization of branchial arches (22). Moreover, maternal insufficiency of vitamin A (the precursor of RA) or RA in excess in vertebrates cause a wide range of teratologic effects (18, 57, 58). All this evidence demonstrates that vertebrates require a precisely regulated supply of retinoids during embryogenesis.

Considering that the phenotypes obtained in our analysis predominantly resemble those of RA excess, we wondered if GBH treatments are able to increase endogenous RA activity. To answer this question, we measured the levels of RA signaling by taking advantage of the reporter plasmid RAREZ (32), as described in the Experimental Procedures section. Figure 4A shows that GBH treatment significantly increased the level of RA signaling in the embryo in a concentration-dependent manner. Importantly, the RA receptor antagonist Ro rescued the effect of GBH since the level of the RA output, as measured by the reporter assay, was not significantly different from that in RAREZ-injected, untreated controls (Figure 4A). Together, these observations strongly suggest that GBH increases endogenous retinoid activity.

If an increase of RA signaling underlies the phenotype produced by GBH treatments, antagonizing the RA pathway should rescue the effect of GBH. To examine this hypothesis, embryos were incubated at the 2-cell stage with GBH alone or with GBH together with 0.5 or 1 µM Ro added when sibling controls reached stage 9 (22). Frog embryos were analyzed by their morphological aspect and also were hybridized with *shh* and *otx2* probes.

Control embryos showed an expression of *otx2* in the forebrain, midbrain, and optic vesicle, while *shh* transcripts are distributed along the embryonic dorsal midline (Figure 4B). Embryos treated continuously with GBH showed a down-regulation of *shh* and *otx2*, reduced head structures, and shortened A-P axis (Figure 4C). Similar results were obtained after treating frog embryos with 0.1 or 1 µM RA (21, 59, 60). As previously reported (22), embryos incubated with 0.5 or 1 µM Ro alone also displayed a concentration-dependent shortening of the A-P axis and reduction of head structures, which was confirmed by a reduction of the *otx2* domain (Figure 4D,E; compare the space between bars with B). We also observed a more diffuse staining of *shh*, mainly in the prechordal meso-derm, in comparison with that of sibling controls (Figure 4D,E; arrows). When 0.5 or 1 µM Ro was added at stage 9 to embryos continuously exposed to 1/5000 dilution of GBH, the elongation of the A-P axis was recovered as well as the normal expression pattern of *otx2* and *shh* (Figure 4F,G). We conclude that the ability of Ro treatment to rescue the teratogenic effect of the GBH supports the idea that RA activity is elevated in GBH-treated embryos.

GBH Produces Similar Teratogenic Effects in Chick Embryos. To test whether the teratogenic effects of GBH are reproducible in an amniote vertebrate, we chose the chick model. Embryos were incubated with 1/3500 or 1/4500 dilutions of GBH and analyzed at the HH stage 9 (8 somites) by immun-ofluorescence with an anti-Pax6 antibody and by WMISH with a *c-shh* probe (61). As was previously demonstrated for Pax6 mRNA (62), the Pax6 protein is normally distributed in the optic vesicle; in the distinctive comet-like shape in the ectoderm, posterior to the region of the optic vesicle; in the hindbrain in rhombomeres r3 and r5 and along the spinal cord (Figure 5A,D). GBH treatments produced a concentration-dependent reduction
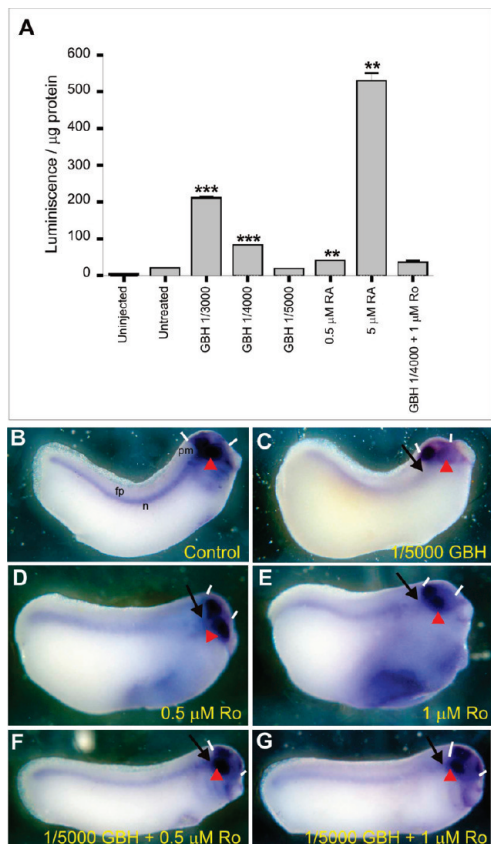
Figure 4. Phenotype induced by GBH is mediated by an increase of RA signaling (A). Analysis of RA activity with the reporter plasmid RAREZ. All embryos were injected with the reporter plasmid RAREZ, except for uninjected controls, and left untreated or were treated as indicated in the figure until stage 14−15, when they were processed. Results are expressed as arbitrary luminescence units per μg of protein. A two-tailed t test was employed to analyze the significance in the difference of the means. ** $p < 0.01$; *** $p < 0.0001$. (B-G) WMISH for *shh* and *otx2* at tailbud stages. (B) Control embryo. Notochord (n); floor plate (fp); brain (space between bars); eye (arrowhead). (C) Embryo treated with 1/5000 GBH manifesting microcephaly (space between bars), reduced eyes (arrowhead), diminished Shh signaling from the prechordal mesoderm (arrow), and shortened A-P axis (78%, $n = 9$). (D,E) Embryos incubated with 0.5 and 1 μM RA antagonist Ro 41-5253, displaying a reduction in the *otx2* domain accompanied by microcephaly (bars) and microphtalmy (arrowhead), and more diffuse expression of *shh* (arrows) (80%, $n = 15$ for 0.5 μM Ro; 87%, $n = 15$ for 1 μM Ro). (F,G) Embryos treated with 1/5000 GBH at the 2-cell stage; 0.5 μM Ro (F) or 1 μM Ro (G) was added at stage 9, and phenotypes were analyzed at the tailbud stage. Notice that Ro reverts the phenotype produced by GBH, rescuing the A-P axis elongation and the expression of *shh* and *otx2* (compare with the control embryo in B) (88%, $n = 17$ for 0.5 μM Ro, which gives the best rescue effect since the effect of the retinoid antagonist begins to prevail with 1 μM Ro). All embryos are oriented with the anterior end toward the right.

of the optic vesicles, as revealed by a reduction of the corresponding Pax6 domain, and this was accompanied by microcephaly (compare the space between bars in Figure 5B,C with A). We also observed a gradual loss of the r3 and r5 domains in embryos treated with GBH (compare Figure 5E,F with D), which resembles the results observed in frog embryos in the *krox-20* domains (Figures 1B and 2E). Hybridization with the *c-shh* probe showed that, as in *Xenopus*, the prechordal mesoderm domain is preferentially lost in GBH-treated chick embryos (compare Figure 5G with H,I). As the GBH concentration increases, the expression along the embryonic dorsal midline also gradually disappears (Figure 5H,I).
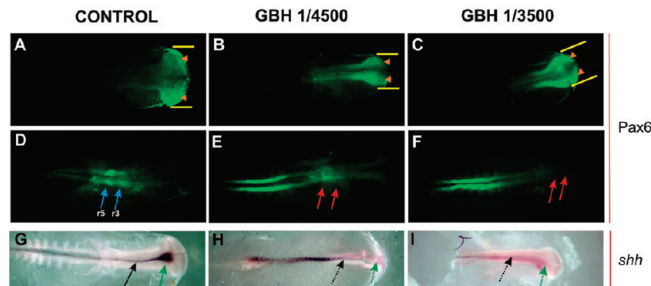

Figure 5. Teratogenic effects of GBH in chicken embryos. (A−C) Whole-mount inmunofluorescence analysis of Pax6 at 8 somites. (A,D) Control embryo showing Pax6 expression in the optic vesicles (arrowheads in A) and in rhombomeres r3 and r5 (blue arrows in D). (B,E and C,F) graded reduction of Pax6 expression in embryos treated with 1/4500 and 1/3500 dilutions of GBH, respectively. Notice the progressive microcephaly (compare space between bars with D) and the loss of Pax6 expression corresponding to rhombomeres r3 and r5 (red arrows). The remaining fluorescence corresponds to specific Pax6 expression that is normally found in the spinal cord but is out of focus in the control embryo in D. (G−I) WMISH with *c-shh*. (G) Control embryo. *Shh* transcripts are seen in dorsal midline cells (black arrow) and in the prechordal mesoderm (green arrow). (H,I) Embryos treated with 1/4500 and 1/3500 dilutions of GBH, respectively. Notice the abolishment of *shh* expression in the prechordal mesoderm (dotted green arrow) and the progressive decrease of *shh* expression in the midline cells in a concentration-dependent manner (dotted black arrows).

Therefore, our experiments with chick embryos further extend conclusions from studies about the teratogenic effects of GBH in amphibians to other vertebrate species.

Discussion

The results presented above argue that both GBH and glyphosate itself interfere with key molecular mechanisms regulating early development in both *Xenopus* and chicken embryos, leading to congenital malformations. Sublethal doses of the herbicide (430 μM of glyphosate in 1/5000 dilutions of GBH) and injections leading to a final concentration of 8 to 12 μM of glyphosate in the injected side of the embryo were sufficient to induce serious disturbances in the expression of *slug*, *otx2*, and *shh*. These molecular phenotypes were correlated with a disruption of developmental mechanisms involving the neural crest, embryonic dorsal midline formation, and cephalic patterning. Because glyphosate penetration through the cell membrane requires facilitation by adjuvants present in commercial formulations (*5, 6*), we tested the effects of glyphosate alone by directly microinjecting it into *Xenopus* embryos. The similarity of the phenotypes obtained in both situations suggests that they are attributable to the active principle of GBH and not to the adjuvants.

We will discuss our results in the following context: (1) the correlation of our phenotypes with those observed in animal models with an impairment of RA signaling or deficits in the expression of critical genes that control embryonic development; (2) the probable mechanisms underlying the phenotypes induced by GBH and glyphosate; (3) possible correlations with clinical cases of human offspring exhibiting malformations in zones exposed to GBH.

Misregulation of RA, *shh*, and *otx2* Are Involved in Cephalic Malformations and Neural Crest-Derived Phenotypes Reminiscent of the Effects of GBH and Glyphosate. The phenotypes obtained after GBH treatments or injections of glyphosate alone are strikingly reminiscent of those observed as a consequence of an excess of RA signaling in vertebrates and humans. Acute or chronic increase of RA levels leads to teratogenic effects during human pregnancy and in experimental

models. The characteristic features displayed by RA embryopathy in humans include brain abnormalities such us microcephaly, microphthalmia, and impairment of hindbrain development; abnormal external and middle ears (microtia or anotia); mandibular and midfacial underdevelopment; and cleft palate. Many craniofacial malformations can be attributed to defects in cranial neural crest cells (*19, 24*).

This spectrum is consistent with the phenotypes obtained in rodent models exposed to RA. When administered during gastrulation in mice, RA severely impairs the development of the anterior neural plate, resulting in ocular, brain, and facial malformations. Exposure at critical stages of neural crest cell migration induces craniofacial malformations comparable to those seen in Di-George syndrome. Later exposure, when the epibranchial placodes are active, results in mandibulofacial dysostosis-like syndromes (*19*). These authors suggest that excessive cell death in regions where apoptosis normally takes place may underlie a general mechanism for craniofacial malformations associated with teratogens.

An excess of RA signaling is able to down-regulate *shh* expression in the embryonic dorsal midline in *Xenopus* (*60, 63*). *Shh* deficiency is associated with holoprosencephaly syndrome (HPE), a CNS malformation with a frequency of 1/250 of pregnancies and 1/10000 of live births. HPE is a defect generated by the deficiency of the embryonic dorsal midline, leading to a failure in the division of the brain hemispheres. This results in unilobar brain, cyclopia, and defects in the closure of the dorsal neural tube, accompanied by other defects including microcephaly, abnormally decreased distance between the eyes (hypotelorism), proboscis, and cebocephaly (a simple nose) (*51−53*). Moreover, Shh signaling is necessary for the development of the cranial neural crest derivatives. In the mouse, specific removal of Shh responsiveness in the neural crest cells that give rise to skeleton and connective tissue in the head increases apoptosis and decreases proliferation in the branchial arches, leading to facial truncations (*64*). In zebrafish, the cranial neural crest requires Shh signaling emanating from the embryonic dorsal midline and the oral ectoderm to achieve correct migration and chondrogenesis (*65*). In chicken embryos, development of the lower jaw skeleton requires Shh signaling from the foregut endoderm to prevent apoptosis of the neural crest cells that migrate to the first branchial arch (*66*). Shh signaling from the ventral midline is necessary, as an antiapoptotic agent, for the survival of the neural epithelium, and it is also essential for the rapid and extensive expansion of the early vesicles of the developing midbrain and forebrain (*67−69*).

An excess of RA signaling also down-regulates *otx2* expression in *Xenopus*, chicken, and mouse embryos (*24*). Knockout mice for *otx2* lack all the brain structures anterior to rhombomere 3. Interestingly, heterozygous mutants showed craniofacial malformations including the loss of the eyes and lower jaw (agnathia). These phenotypes are reminiscent of otocephaly reported in humans and other animals and suggest that *otx2* plays an essential role in the development of cranial skeletons of mesencephalic neural crest origin (*70−72*).

Otx2, in turn, is necessary for the expression of *shh* in the ventral midbrain (*73*). All this evidence indicates that RA signaling, *otx2*, and *shh* are part of a genetic cascade critical for the development of the brain and craniofacial skeleton of neural crest origin. Glyphosate inhibits the anterior expression of *shh*, reduces the domain of *otx2*, prevents the subdivision of the eye field, and impairs craniofacial development, resembling aspects of the holoprensecephalic and otocephalic syndromes.

This prompted us to investigate whether an increase of RA signaling could be mediating the effects of GBH treatments.

GBH Increases the Activity of the Morphogen RA, Leading to Teratogenic Effects. In *Xenopus* embryos, the endogenous activity of retinoids gradually increases during early embryogenesis and is finely regulated in space. At late gastrula, a rostral−caudal gradient from 0.01 to 0.16 μM RA is established, with the highest levels at the posterior end of the embryo. The gradient persists at the early neurula stage (stage 13−14). Synthesis and degradation of RA seem to be the mechanisms that lead to this uneven distribution (*74*). This gradient explains why low doses of applied RA primarily affect the cephalic region and increasing the doses begins to affect the trunk (*20, 21*). Moreover, maintaining a normal endogenous distribution of RA is important for axes patterning and organogenesis not only in *Xenopus* (*74, 22, 38*) but also in other Vertebrates such as zebrafish (*75−77*), chicken (*78−80*), and mouse embryos (*81*).

In this study, GBH treatments or glyphosate injections mostly reproduce the morphological phenotype obtained after treatments of *Xenopus* embryos with RA concentrations from 0.1 to 10 μM (*21*). The fact that GBH treatments increase endogenous RA activity, as measured by the RAREZ reporter, and that the GBH-induced phenotypes are rescued by the antiretinoid Ro strongly suggest that augmented RA activity is a major cause of the molecular and morphological phenotypes described in this work.

GBHs are considered endocrine disruptors because of their ability to impair the synthesis of steroid hormones (*82*). Glyphosate inhibits the activity of aromatase, a member of the cytochrome P450 family crucial for sex steroid hormone synthesis (*4*). Retinoid activity is regulated by degradation of RA by the CYP26 enzymes, which are members of the cytochrome P450 family and are present in all vertebrates from early stages of embryogenesis. Transcription of CYP26 is developmentally and spatially regulated. Deficiencies of this enzyme produce serious malformations in different vertebrate models consistent with an important increase in RA signaling. These phenotypes include cephalic defects, abnormalities of the eye and the forebrain, agnathia, and caudal truncations (*83−90*). In this context, it will be interesting to elucidate in the future if the increase of RA signaling induced by GBH could be a consequence of inhibiting the activity of CYP26 enzymes responsible for maintaining a normal RA distribution by specific territorial degradation.

In *Xenopus laevis*, RA favors the differentiation of primary neurons (*39, 60, 91*). Since GBH increases retinoid signaling, the reduction in the number of primary neurons in GBH-treated and glyphosate-injected embryos is paradoxical. Other biochemical mechanisms could be triggering the inhibition of neurogenesis. For example, we cannot rule out that apoptosis of neural precursors could be involved in this process since GBH and glyphosate have a toxic effect on mitochondrial membranes and activate caspases3/7 (*7*). Both GBH and glyphosate inhibit *shh* expression, and the Shh protein is known to have an antiapoptotic function, necessary for the survival of the neuroepithelium (*67, 68*). Abnormal induction of cell death is one of the crucial mechanisms of malformations associated with different teratogenic agents such as ethanol, RA, hypoxia, and chemicals herbicides (*19, 92*).

Assuming a linear response of the luminescence system with the RAREZ reporter used to measure RA signaling, we estimate that the endogenous concentration of RA available for activity in *Xenopus* embryos is around 0.2 μM (Figure 4A, compare

RA bars with the RAREZ bar). This is very similar to the average concentration of 0.15 μM previously measured by HPLC (*20*). Importantly, treatments with 1/5000 dilution of GBH do not show a significant increase of RA activity when compared to that of untreated controls, as measured by the reporter system (Figure 4A). However, this dilution clearly produces cephalic and trunk phenotypes and craniofacial malformations, as shown throughout this work, which are rescued by Ro treatments. Therefore, the RAREZ reporter does not seem to be sensitive enough to detect minimal variations in the levels of RA activity. This reinforces the importance of using vertebrate embryos as biosensors for testing possible teratogens.

Moreover, it has been recently reported that Triadimefon, a systemic fungicide with teratogenic effects in rodent models, produces craniofacial malformations in *Xenopus laevis* by altering endogenous RA signaling (*93*). Arsenic, another endocrine disruptor, also increases RA signaling at low, noncytotoxic doses, in human embryonic NT2 cells (*94*). RA signaling is one of the finest pathways to tune up gene regulation during development, and all this evidence raises the possibility that disturbances in RA distribution may be a more general mechanism underlying the teratogenic effects of xenobiotics in vertebrates. Since mechanisms of development are highly conserved in evolution among vertebrates (*95*), we would like to stress that they could be useful as very sensitive biosensors to detect the undesirable effects of new molecules.

Clinical Approaches. In Argentina, the extension of soil devoted to transgenic soy reached 19 million hectares. Two hundred million liters of glyphosate-based herbicide is used for a production of 50 million tons of soy beans per year (*96, 97*). The intensive and extensive agricultural models based on the GMO technological package are currently applied without critical evaluation, rigorous regulations, and adequate information about the impact of sublethal doses on human health and the environment, leading to a conflicting situation. In this work, we focused on sublethal doses of GBH to arrive at the thresholds for teratogenic phenotypes instead of lethality.

In the last 10 years, several countries in Latin America have initiated studies about the environmental consequences of the use of herbicides and pesticides. In Paraguay, an epidemiological study in the offspring of women exposed during pregnancy to herbicides showed 52 cases of malformations (*3*), which strikingly resemble the wide spectrum phenotypes resulting from a dysfunctional RA or Shh signaling pathway. In Argentina, an increase in the incidence of congenital malformations began to be reported in the last few years (Dr. Hugo Lucero, Universidad Nacional del Nordeste, Chaco; personal communication). In Córdoba, several cases of malformations together with repeated spontaneous abortions were detected in the village of Ituzaingó, which is surrounded by GMO-based agriculture. These findings were concentrated in families living a few meters from where the herbicides are regularly sprayed. All of this information is extremely worrying because the risk of environmentally-induced disruptions in human development is highest during the critical period of gestation (2 to 8 weeks) (*98*). Moreover, the mature human placenta has been shown to be permeable to glyphosate. After 2.5 h of perfusion, 15% of administered glyphosate is transferred to the fetal compartment (*99*).

All of the evidence reported in the scientific literature and the clinical observations in the field were not sufficient, however, to activate the precautionary principle of the environmental legislation in order to realize the depth of the impact on human health produced by herbicides in GMO-based agriculture. To our knowledge, the results presented in this work show for the first time that at least some of the malformations produced by GBH in vertebrate embryos are due to an increase of endogenous RA activity, consistent with the well-known syndrome produced by an excess of RA.

References

(1) vom Saal, F., and Hughes, C. (2005) An extensive new literature concerning low-dose effects of bisphenol A shows the need for a new risk assessment. *Environ. Health Perspect. 113*, 926–933.

(2) Myers, J., Zoeller, R., and vom Saal, F. (2009) A clash of old and new scientific concepts in toxicity, with important implications for public health. *Environ. Health Perspect. 117*, 1652–1655.

(3) Benítez Leite, S., Macchi, M. A., and Acosta, M. (2009) Malformaciones Congénitas asociadas a agrotóxicos. *Arch. Pediatr. Drug 80*, 237–247.

(4) Richard, S., Moslemi, S., Sipahutar, H., Benachour, N., and Seralini, G. E. (2005) Differential effects of glyphosate and roundup on human placental cells and aromatase. *Environ Health Perspect 113*, 716–720.

(5) Haefs, R., Schmitz-Eiberger, M., Mainx, H. G., Mittelstaedt, W., and Noga, G. (2002) Studies on a new group of biodegradable surfactants for glyphosate. *Pest. Manag. Sci. 58*, 825–833.

(6) Marc, J., Mulner-Lorillon, O., Boulben, S., Hureau, D., Durand, G., and Belle, R. (2002) Pesticide Roundup provokes cell division dysfunction at the level of CDK1/cyclin B activation. *Chem. Res. Toxicol. 15*, 326–331.

(7) Benachour, N., and Seralini, G. E. (2009) Glyphosate formulations induce apoptosis and necrosis in human umbilical, embryonic, and placental cells. *Chem. Res. Toxicol. 22*, 97–105.

(8) Gasnier, C., Dumont, C., Benachour, N., Clair, E., Chagnon, M. C., and Seralini, G. E. (2009) Glyphosate-based herbicides are toxic and endocrine disruptors in human cell lines. *Toxicology 262*, 184–191.

(9) Spiroux de Vendômôis, J., Roullier, F., Cellier, D., and Seralini, G. E. (2009) A comparison of the effects of three GM corn varieties on mammalian health. *Int. J. Biol. Sci. 5*, 706–726.

(10) Marc, J., Mulner-Lorillon, O., and Belle, R. (2004) Glyphosate-based pesticides affect cell cycle regulation. *Biol. Cell 96*, 245–249.

(11) Bellé, R., Le, B. R., Morales, J., Cosson, B., Cormier, P., and Mulner-Lorillon, O. (2007) Sea urchin embryo, DNA-damaged cell cycle checkpoint and the mechanisms initiating cancer development. *J. Soc. Biol. 201*, 317–327.

(12) Marc, J., Belle, R., Morales, J., Cormier, P., and Mulner-Lorillon, O. 2004b Formulated glyphosate activates the DNA-response checkpoint of the cell cycle leading to the prevention of G2/M transition. *Toxicol. Sci. 82*, 436–442.

(13) Mañas, F., Peralta, L., Raviolo, J., Garcia, O. H., Weyers, A., Ugnia, L., Gonzalez, C. M., Larripa, I., and Gorla, N. 2009a Genotoxicity of AMPA, the environmental metabolite of glyphosate, assessed by the Comet assay and cytogenetic tests. *Ecotoxicol. Environ. Saf. 72*, 834–837.

(14) Mañas, F., Peralta, L., Raviolo, J., Garcia, O. H., Weyers, A., Ugnia, L., Gonzalez, C. M., Larripa, I., and Gorla, N. 2009b Genotoxicity of glyphosate assessed by the comet assay and cytogenetic tests. *Environ. Toxicol. Pharmacol. 28*, 37–41.

(15) Lajmanovich, R. C., Sandoval, M. T., and Peltzer, P. M. (2003) Induction of mortality and malformation in Scinax nasicus tadpoles exposed to glyphosate formulations. *Bull. Environ. Contam. Toxicol. 70*, 612–618.

(16) Apfel, C., Bauer, F., Crettaz, M., Forni, L., Kamber, M., Daufmann, F., LeMotte, P., Pirson, M., and Klaus, M. (1992) A retinoic acid receptor á antagonist selectively counteracts retinoic acid effects. *Proc. Natl. Acad. Sci. U.S.A. 89*, 7129–7133.

(17) Moroni, M., Vigano, M., and Mavilio, F. (1993) Regulation of the human HOXD4 gene by retinoids. *Mech. Dev. 44*, 139–154.

(18) Lammer, E. J., Chen, D. T., Hoar, R. M., Agnish, N. D., Benke, P. J., Braun, J. T., Curry, C. J., Fernhoff, P. M., Jr., Lott, I. T., et al. (1985) Retinoic acid embryopathy. *N. Engl. J. Med. 313*, 837–841.

(19) Sulik, K. K., Cook, C. S., and Webster, W. S. (1988) Teratogens and craniofacial malformations: relationships to cell death. *Development 103* (Suppl.), 213–231.

(20) Durston, A. J., Timmermans, J. P., Hage, W. J., Hendriks, H. F., de Vries, N. J., Heideveld, M., and Nieuwkoop, P. D. (1989) Retinoic acid causes an anteroposterior transformation in the developing central nervous system. *Nature 340*, 140–144.

(21) López, S. L., and Carrasco, A. E. (1992) Retinoic acid induces changes in the localization of homeobox proteins in the antero-posterior axis of *Xenopus laevis* embryos. *Mech. Dev. 36*, 153–164.

(22) López, S. L., Dono, R., Zeller, R., and Carrasco, A. E. (1995) Differential effects of retinoic acid and a retinoid antagonist on the spatial distribution of the homeoprotein Hoxb-7 in vertebrate embryos. *Dev. Dyn. 204*, 457–471.

(23) Clotman, F., van Maele-Fabry, G., and Picard, J. J. (1997) Retinoic acid induces a tissue-specific deletion in the expression domain of Otx2. *Neurotoxicol. Teratol. 19*, 163–169.

(24) Clotman, F., van Maele-Fabry, G., Chu-Wu, L., and Picard, J. J. (1998) Structural and gene expression abnormalities induced by retinoic acid in the forebrain. *Reprod. Toxicol. 12*, 169–176.

(25) Padmanabhan, R. (1998) Retinoic acid-induced caudal regression syndrome in the mouse fetus. *Reprod. Toxicol. 12*, 139–151.

(26) Gurdon, J. (1976) Injected nuclei in frog oocytes: Fate, enlargement, and chromatin dispersal. *J. Embryo Exp. Morphol. 36*, 523–540.

(27) Nieuwkoop, P., Faber, J. (1994) *Normal Table of Xenopus laevis (Daudin)*, Garland Publishing, Inc., New York.

(28) Harland, R. (1991) In situ hybridization: an improved whole mount method for *Xenopus* embryos. *Methods Cell Biol. 36*, 685–695.

(29) Revinski, D. R., Paganelli, A. R., Carrasco, A. E., and López, S. L. (2010) Delta-Notch signaling is involved in the segregation of the three germ layers in *Xenopus laevis*. *Dev. Biol. 339*, 477–492.

(30) Pizard, A., Haramis, A., Carrasco, A. E., Franco, P., López, S., and Paganelli, A. (2004) Whole-Mount in Situ Hybridization and Detection of RNAs in Vertebrate Embryos and Isolated Organs, in *Current Protocols in Molecular Biology* (Ausubel, F. M., Eds.) pp 14.9.1–14.9.24, Wiley, New York.

(31) Rossant, J., Zirngibl, R., Cado, D., Shago, M., and Giguère, V. (1991) Expression of a retinoic acid response element-hsplacZ transgene defines specific domains of transcriptional activity during mouse embryogenesis. *Genes Dev. 5*, 1333–1344.

(32) Kot-Leibovich, H., and Fainsod, A. (2009) Ethanol induces embryonic malformations by competing for retinaldehyde dehydrogenase activity during vertebrate gastrulation. *Dis. Model Mech. 2*, 295–305.

(33) Lowry, O. H., Rosebrough, N. J., Farr, A. L., and Randall, R. J. (1951) Protein measurement with the Folin phenol reagent. *J. Biol. Chem. 193*, 265–275.

(34) Hamburger, V., and Hamilton, H. L. (1951) A series of normal stages in the development of the chick emhryo. *J. Morphol. 88*, 49–92.

(35) Mayor, R., Morgan, R., and Sargent, M. G. (1995) Induction of the prospective neural crest of Xenopus. *Development 121*, 767–777.

(36) Bradley, L. C., Snape, A., Bhatt, S., and Wilkinson, D. G. (1993) The structure and expression of the *Xenopus* Krox-20 gene: conserved and divergent patterns of expression in rhombomeres and neural crest. *Mech. Dev. 40*, 73–84.

(37) Murphy, P., Davidson, D. R., Hill, R. E., and Morriss-Kay, G. M. (1992) Retinoid-Induced Alterations of Segmental Organization and Gene Expression in the Mouse Hindbrain, in *Retinoids in Normal Development and Teratogenesis* (Morriss-Kay, G., Ed.), pp 229–240, Oxford University Press, Oxford, U.K.

(38) Godsave, S. F., Koster, C. H., Getahun, A., Mathu, M., Hooiveld, M., van der Wees, J., Hendriks, J., and Durston, A. J. (1998) Graded retinoid responses in the developing hindbrain. *Dev. Dyn. 213*, 39–49.

(39) Papalopulu, N., and Kintner, C. (1996) A posteriorising factor, retinoic acid, reveals that anteroposterior patterning controls the timing of neuronal differentiation in *Xenopus* neuroectoderm. *Development 122*, 3409–3418.

(40) Sadaghiani, B., and Thiébaud, C. H. (1987) Neural crest development in the *Xenopus laevis* embryo, studied by interspecific transplantation and scanning electron microscopy. *Dev. Biol. 124*, 91–110.

(41) López, S., and Carrasco, A. E. (2005) Sonic Hedgehog Signalling in Dorsal Midline Development, in *Shh and Gli Signaling and Development* (Howie, S., and Fisher, C., Eds.) Chapter 1, p 111. Landes Bioscience, Austin, TX.

(42) Varjosalo, M., and Taipale, J. (2008) Hedgehog: functions and mechanisms. *Genes Dev. 22*, 2454–2472.

(43) Li, H., Tierney, C., Wen, L., Wu, J. Y., and Rao, Y. (1997) A single morphogenetic field gives rise to two retina primordia under the influence of the prechordal plate. *Development 124*, 603–615.

(44) Walther, C., and Gruss, P. (1991) Pax-6, a murine paired box gene, is expressed in the developing CNS. *Development 113*, 1435–1449.

(45) Krauss, S., Johanson, T., Korzh, V., and Fjose, A. (1991) Expression pattern of zebrafish pax genes suggest a role in early brain regionalization. *Nature 353*, 267–270.

(46) Püschel, A. W., Gruss, P., and Westerfield, M. (1992) Sequence and expression pattern of *pax-6* are highly conserved between zebrafish and mice. *Development 114*, 643–651.

(47) Glaser, T., Jepeal, L., Edwards, J. G., Young, S. R., Favor, J., and Maas, R. L. (1994) *Pax6* gene dosage effect in a family with congenital cataracts, aniridia, anophthalmia and central nervous system defect. *Nat. Genet. 7*, 463–471.

(48) Pannese, M., Polo, C., Andreazzoli, M., Vignali, R., Kablar, B., Barsacchi, G., and Boncinelli, E. (1995) The *Xenopus* homologue of Otx2 is a maternal homeobox gene that demarcates and specifies anterior body regions. *Development 121*, 707–720.

(49) Zygar, C. A., Cook, T. L., and Grainger, R. M. (1998) Gene activation during early stages of lens induction in *Xenopus*. *Development. 125*, 3509–3519.

(50) Spokony, R. F., Aoki, Y., Saint-Germain, N., Magner-Fink, E., and Saint-Jeannet, J. P. (2002) The transcription factor Sox9 is required for cranial neural crest development in *Xenopus*. *Development 129*, 421–432.

(51) Chiang, C., Litingtung, Y., Lee, E., Young, K. E., Corden, J. L., Westphal, H., and Beachy, P. A. (1996) Cyclopia and defective axial patterning in mice lacking Sonic hedgehog gene function. *Nature 383*, 407–413.

(52) Roessler, E., Belloni, E., Gaudenz, K., Jay, P., Berta, P., Scherer, S. W., Tsui, L. C., and Muenke, M. (1996) Mutations in the human Sonic hedgehog gene cause holoprosencephaly. *Nat. Genet. 14*, 357–360.

(53) Chen, J. K., Taipale, J., Cooper, M. K., and Beachy, P. A. (2002) Inhibition of Hedgehog signaling by direct binding of cyclopamine to Smoothened. *Genes Dev. 16*, 2743–2748.

(54) Mark, M., Ghyselinck, N. B., and Chambon, P. (2006) Function of retinoid nuclear receptors: lessons from genetic and pharmacological dissections of the retinoic acid signaling pathway during mouse embryogenesis. *Annu. Rev. Pharmacol. Toxicol. 46*, 451–480.

(55) Blumberg, B., Mangelsdorf, D. J., Dyck, J. A., Bittner, D. A., Evans, R. M., and De Robertis, E. M. (1992) Multiple retinoid-responsive receptors in a single cell: families of retinoid "X" receptors and retinoic acid receptors in the *Xenopus* egg. *Proc. Natl. Acad. Sci. U.S.A. 89*, 2321–2325.

(56) Sharpe, C. R. (1992) Two isoforms of retinoic acid receptor alpha expressed during *Xenopus* development respond to retinoic acid. *Mech. Dev. 39*, 81–93.

(57) Lammer, E. J., and Armstrong, D. L. (1992) Malformations of Hindbrain Structures among Humans Exposed to Isotretinoin (13-*cis*-Retinoic Acid) during Early Embryogenesis, in *Retinoids in Normal Development and Teratogenesis* (Morriss-Kay, G., Ed.) pp 281–295, Oxford University Press, Oxford, U.K.

(58) Ross, S. A., McCaffery, P. J., Drager, U. C., and De Luca, L. M. (2000) Retinoids in embryonal development. *Physiol. Rev. 80*, 1021–1054.

(59) Andreazzoli, M., Pannese, M., and Boncinelli, E. (1997) Activating and repressing signals in head development: the role of Xotx1 and Xotx2. *Development. 124*, 1733–1743.

(60) Franco, P. G., Paganelli, A. R., López, S. L., and Carrasco, A. E. (1999) Functional association of retinoic acid and hedgehog signaling in *Xenopus* primary neurogenesis. *Development 126*, 4257–4265.

(61) Riddle, R. D., Johnson, R. L., Laufer, E., and Tabin, C. (1993) Sonic hedgehog mediates the polarizing activity of the ZPA. *Cell 75*, 1401–1416.

(62) Li, H. S., Yang, J. M., Jacobson, R. D., Pasko, D., and Sundin, O. (1994) Pax-6 is first expressed in a region of ectoderm anterior to the early neural plate: implications for stepwise determination of the lens. *Dev. Biol. 162*, 181–194.

(63) Sharpe, C., and Goldstone, K. (2000) Retinoid signalling acts during the gastrula stages to promote primary neurogenesis. *Int. J. Dev. Biol.* *44*, 463–470.

(64) Jeong, J., Mao, J., Tenzen, T., Kottmann, A. H., and McMahon, A. P. (2004) Hedgehog signaling in the neural crest cells regulates the patterning and growth of facial primordia. *Genes Dev. 18*, 937–951.

(65) Wada, N., Javidan, Y., Nelson, S., Carney, T. J., Kelsh, R. N., and Schilling, T. F. (2005) Hedgehog signaling is required for cranial neural crest morphogenesis and chondrogenesis at the midline in the zebrafish skull. *Development 132*, 3977–3988.

(66) Brito, J. M., Teillet, M. A., and Le Douarin, N. M. (2006) An early role for sonic hedgehog from foregut endoderm in jaw development: ensuring neural crest cell survival. *Proc. Natl. Acad. Sci. U.S.A. 103*, 11607–11612.

(67) Le Douarin, N. M., and Halpern, M. E. (2000) Discussion point. Origin and specification of the neural tube floor plate: insights from the chick and zebrafish. *Curr. Opin. Neurobiol. 10*, 23–30.

(68) Charrier, J. B., Lapointe, F., Le Douarin, N. M., and Teillet, M. A. (2001) Anti-apoptotic role of Sonic hedgehog protein at the early stages of nervous system organogenesis. *Development 128*, 4011–4020.

(69) Britto, J., Tannahill, D., and Keynes, R. (2002) A critical role for sonic hedgehog signaling in the early expansion of the developing brain. *Nat. Neurosci. 5*, 103–110.

(70) Matsuo, I., Kuratani, S., Kimura, C., Takeda, N., and Aizawa, S. (1995) Mouse Otx2 functions in the formation and patterning of rostral head. *Genes Dev. 9*, 2646–2658.

(71) Kimura, C., Takeda, N., Suzuki, M., Oshimura, M., Aizawa, S., and Matsuo, I. (1997) Cis-acting elements conserved between mouse and pufferfish Otx2 genes govern the expression in mesencephalic neural crest cells. *Development 124*, 3929–3941.

(72) Erlich, M. S., Cunningham, M. L., and Hudgins, L. (2000) Transmission of the dysgnathia complex from mother to daughter. *Am. J. Med. Genet. 95*, 269–274.

(73) Jin, O., Harpal, K., Ang, S. L., and Rossant, J. (2001) Otx2 and HNF3beta genetically interact in anterior patterning. *Int. J. Dev. Biol. 45*, 357–365.

(74) Chen, Y., Huang, L., and Solursh, M. (1994) A concentration gradient of retinoids in the early *Xenopus laevis* embryo. *Dev. Biol. 161*, 70–76.

(75) Marsh-Armstrong, N., McCaffery, P., Hyatt, G., Alonso, L., Dowling, J. E., Gilbert, W., and Dräger, U. C. (1995) Retinoic acid in the anteroposterior patterning of the zebrafish trunk. *Roux's Arch. Dev. Biol. 205*, 103–113.

(76) Grandel, H., Lun, K., Rauch, G. J., Rhinn, M., Piotrowski, T., Houart, C., Sordino, P., Kuchler, A. M., Schulte-Merker, S., Geisler, R., et al. (2002) Retinoic acid signalling in the zebrafish embryo is necessary during pre-segmentation stages to pattern the anterior-posterior axis of the CNS and to induce a pectoral fin bud. *Development 129*, 2851–2865.

(77) Dobbs-McAuliffe, B., Zhao, Q., and Linney, E. (2004) Feedback mechanisms regulate retinoic acid production and degradation in the zebrafish embryo. *Mech. Dev. 121*, 339–350.

(78) Maden, M. (2000) The role of retinoic acid in embryonic and post-embryonic development. *Proc. Nutr. Soc. 59*, 65–73.

(79) Berggren, K., McCaffery, P., Drager, U., and Forehand, C. J. (1999) Differential distribution of retinoic acid synthesis in the chicken embryo as determined by immunolocalization of the retinoic acid synthetic enzyme, RALDH-2. *Dev. Biol. 210*, 288–304.

(80) Chen, Y., Huang, L., Russo, A. F., and Solursh, M. (1992) Retinoic acid is enriched in Hensen's node and is developmentally regulated in the early chicken embryo. *Proc. Natl. Acad. Sci. U.S.A. 89*, 10056–10059.

(81) Ang, H. L., Deltour, L., Hayamizu, T. F., Zgombic-Knight, M., and Duester, G. (1996) Retinoic acid synthesis in mouse embryos during gastrulation and craniofacial development linked to class IV alcohol dehydrogenase gene expression. *J. Biol. Chem. 271*, 9526–9534.

(82) Walsh, L. P., McCormick, C., Martin, C., and Stocco, D. M. (2000) Roundup inhibits steroidogenesis by disrupting steroidogenic acute regulatory (StAR) protein expression. *Environ. Health Perspect. 108*, 769–776.

(83) de Roos, K., Sonneveld, E., Compaan, B., ten, B. D., Durston, A. J., and van der Saag, P. T. (1999) Expression of retinoic acid 4-hydroxylase (CYP26) during mouse and *Xenopus laevis* embryogenesis. *Mech. Dev. 82*, 205–211.

(84) Maden, M., Sonneveld, E., van der Saag, P. T., and Gale, E. (1998) The distribution of endogenous retinoic acid in the chick embryo: implications for developmental mechanisms. *Development 125*, 4133–4144.

(85) Sakai, Y., Meno, C., Fujii, H., Nishino, J., Shiratori, H., Saijoh, Y., Rossant, J., and Hamada, H. (2001) The retinoic acid-inactivating enzyme CYP26 is essential for establishing an uneven distribution of retinoic acid along the anterio-posterior axis within the mouse embryo. *Genes Dev. 15*, 213–225.

(86) Gongal, P. A., and Waskiewicz, A. J. (2008) Zebrafish model of holoprosencephaly demonstrates a key role for TGIF in regulating retinoic acid metabolism. *Hum. Mol. Genet. 17*, 525–538.

(87) Hernández, R. E., Putzke, A. P., Myers, J. P., Margaretha, L., and Moens, C. B. (2007) Cyp26 enzymes generate the retinoic acid response pattern necessary for hindbrain development. *Development 134*, 177–187.

(88) Reijntjes, S., Rodaway, A., and Maden, M. (2007) The retinoic acid metabolising gene, CYP26B1, patterns the cartilaginous cranial neural crest in zebrafish. *Int. J. Dev. Biol. 51*, 351–360.

(89) Duester, G. (2008) Retinoic acid synthesis and signaling during early organogenesis. *Cell. 134*, 921–931.

(90) Niederreither, K., and Dollé, P. (2008) Retinoic acid in development: towards an integrated view. *Nat. Rev. Genet. 9*, 541–553.

(91) Blumberg, B., Jr., Moreno, T. A., Kintner, C., Evans, R. M., and Papalopulu, N. (1997) An essential role for retinoid signaling in anteroposterior neural patterning. *Development 124*, 373–379.

(92) Ahlgren, S. C., Thakur, V., and Bronner-Fraser, M. (2002) Sonic hedgehog rescues cranial neural crest from cell death induced by ethanol exposure. *Proc. Natl. Acad. Sci. U.S.A. 99*, 10476–10481.

(93) Papis, E., Bernardini, G., Gornati, R., Menegola, E., and Prati, M. (2007) Gene expression in *Xenopus laevis* embryos after Triadimefon exposure. *Gene Exp. Patterns 7*, 137–142.

(94) Davey, J. C., Nomikos, A. P., Wungjiranirun, M., Sherman, J. R., Ingram, L., Batki, C., Lariviere, J. P., and Hamilton, J. W. (2008) Arsenic as an endocrine disruptor: arsenic disrupts retinoic acid receptor-and thyroid hormone receptor-mediated gene regulation and thyroid hormone-mediated amphibian tail metamorphosis. *Environ. Health Perspect. 116*, 165–172.

(95) Stern, C. (2005) *Gastrulation: From Cells to Embryo* (Stern, C. D., Ed.) Cold Spring Harbor Laboratory Press, New York.

(96) Teubal, M., Domínguez, D., Sabatino, P. (2005). Transformaciones agrarias en la argentina. Agricultura industrial y sistema agroalimentario. In: *El campo argentino en la encrucijada. Estrategias y resistencias sociales, ecos en la ciudad.* (ed. Giarracca, N. Teubal, M.), pp 37−78. Buenos Aires: Alianza Ed.ial.

(97) Teubal, M. (2009) Expansión del modelo sojero en la Argentina. De la producción de alimentos a los commodities, in *La persistencia del campesinado en América Latina* (Lizarraga, P., and Vacaflores, C., Eds.) pp 161−197, Comunidad de Estudios JAINA, Tarija.

(98) Gilbert, S. (2003) In *Developmental Biology*, 7th ed., Sinauer Associates, Inc., Sunderland, MA.

(99) Poulsen, M. S., Rytting, E., Mose, T., and Knudsen, L. E. (2009) Modeling placental transport: correlation of in vitro BeWo cell permeability and ex vivo human placental perfusion. *Toxicol. in Vitro 23*, 1380–1386.